LETTER

Enhanced Dielectric Properties of Three-Phase-Percolative Composites Based on Thermoplastic-Ceramic Matrix ($BaTiO_3$ + PVDF) and ZnO Radial Nanostructures

Guangsheng Wang*

Division of Nanomaterials & Chemistry, Hefei National Laboratory for Physical Sciences at Microscale, Department of Chemistry, University of Science and Technology of China, Hefei 230026, P. R. China, and School of Chemistry & Environment, BeiHang University, Beijing 100191, P. R. China.

ABSTRACT Three-phase-percolative composites with ZnO radial nanoclusters (R-ZnO) and $BaTiO_3$ (BT) nanoparticles embedded into polyvinylidene fluoride (PVDF) were prepared by using a simple blending and hot-molding technique. The BT + PVDF composite with a volume fraction of 30 vol % BT particles were employed as a thermoplastic-ceramic matrix. Compared with the two-phase-percolative composites of R-ZnO/PVDF, the three-phase-percolative (R-ZnO/(BT + PVDF)) composites showed enhanced dielectric constant and decreased dielectric loss. The percolation theory was used to explain the experimental results. The increased percolation threshold was studied in detail, and the thermal stability was also investigated.

KEYWORDS: dielectric properties • three-phase-percolative composites • ZnO nanostructures • hot-molding technique • percolation theory • thermal stability

1. INTRODUCTION

The polymer-matrix composites with high dielectric permittivity have received increasing interest recently for various potential applications in high charge-storage capacitor (1). A wide variety of high-dielectric-constant composite materials has been developed. Efforts to improve the overall dielectric performance of these materials have been devoted to maximize the dielectric constant and suppress the dielectric loss. Two methods are currently employed for improving the dielectric constant of the polymers. One is to disperse some ferroelectric ceramic powders into the polymer to form 0−3 type composites. Traditional ceramics, e.g., BT, $BaSrTiO_3$, $PbZrTiO_3$, have been actively explored as fillers (2−8). The effective dielectric constant of the ferroelectric ceramic-polymer composites increases with the volume fraction of the ceramics based on the mixing rules, although the dielectric constant of these polymer-ceramic composites developed to date is below 100 at room temperature.

Other significant efforts have focused on developing percolative composites. Conductive filler/polymer composite is another approach toward high dielectric constant materials, which is a kind of conductor−insulator composite based on percolation theory. Ultrahigh dielectric constant can be expected with conductive filler/polymer composites when the concentration of the conductive filler is approaching the percolation threshold. And also this percolative approach requires much lower volume concentration of the filler compared to traditional approach of high dielectric constant particles in a polymer matrix. Therefore, this material option represents advantageous characteristics over the conventional ceramic/polymer composites. Various conductive fillers, such as silver (Ag), aluminum (Al), nickel (Ni), and carbon black, have been used to prepare the polymer-conductive filler composites or three-phase percolative composite systems (9−16). Although these composites were reported with high dielectric constant, they still cannot be considered as effective materials for embedded capacitor applications because the accompanied high dielectric loss tangent and conductivity.

Although the high dielectric constants of the polymer-based composite are relatively well obtained, the role of the fillers, such as metal and ceramic particles in three-phase composites, remains to be examined. New insights into the unique properties of the nanoparticle filler and polymer-matrix have been gained in most recent studies. For example, by dispersing semiconductor ZnO in the form of radial nanowire clusters structure into the PVDF, we obtained a high dielectric constant in the neighborhood of the percolation threshold (17). The percolation threshold concentration of the ZnO is low as 5.48 (vol %). However, for the percolation composite, the dielectric constants decrease rapidly with the increasing frequency and the dielectric loss increases rapidly too; the dielectric loss is greater than 0.5 in the low frequency. From a dielectric property point of view, dielectric constant and dielectric loss are the two most important parameters that dictate the performance of a candidate material for embedded capacitors. How to in-

* Corresponding author. E-mail: wanggsh@ustc.edu.cn.
Received for review April 1, 2010 and accepted April 21, 2010
DOI: 10.1021/am100296u

Published on Web 04/23/2010

crease the dielectric constant and decrease the dielectric loss is still a challenge. Here, ZnO powders with radial nanostructures (R-ZnO) were added as the third phase into thermoplastic-ceramic matrix (BT + PVDF) to get a higher dielectric constant of the composites and lower dielectric loss.

2. EXPERIMENTAL SECTION

Commercially available and analytical-grade reagents were used without further purification. 1.1 g of $Zn(CH_3COO)_2 \cdot 2H_2O$ was dissolved in a 150 mL solution of xylene and glycol with a volume ratio R_v (V_{xylene}/V_{glycol}) 15; some dodecyl benzene sulfonic acid sodium (DBS) with a molar ratio R_D [R_D = (DBS/$Zn(CH_3COO)_2 \cdot 2H_2O$)] of 0.85 was then added in succession. After the solution was vigorously stirred for 1 h at room temperature, 50% hydrate hydrazine was added to the solution and refluxed for another 5 h. The white precipitates were then collected, washed with ethanol and distilled water several times, and then dried in the oven at 70 °C.

The composites were prepared by mixing the BT powders (80−100 nm) with the polymer PVDF using a simple blending and hot-molding procedure. PVDF was dissolved in *N*-dimethylformamide (DMF) at room temperature. After the solution was transparent, various contents of R-ZnO were added and then dispersed in fosters after the ultrasonic bath at room temperature. After that, it was dried in the oven at 100 °C. The dried mixture was collapsed and compressed into wafers for 15 min at 200 °C under 10 MPa (prepressed for 5 min at the same temperature, released the press for a while, and then repressed for 20 min, followed by cooling to room temperature under the same pressure).

Powder XRD data were collected on a Rigaku D/MAX 2200 PC automatic X-ray diffractometer with Cu Ka radiation (λ = 0.154056 nm). The grain morphology and size was observed by SEM (FEI Siron 200). The dielectric constants are measured by a HP 4294A Impedance meter in the frequency range of 100/11 MHz, at an average voltage of 0.5 V from 20 to 140 °C temperature.

3. RESULTS AND DISCUSSION

The redial nanostructure was studied in ref 17 and summarized as follows: the radial ZnO nanowires possess a single-crystal hexagonal structure, which grow on a hexagonal prism tip and there exists a clear crystal boundary between nanowires and the prism. The diameter of radial ZnO nanowires at the top is about 50 nm and the length is from 400 nm to 2 μm, whereas the diameter and length of the hexagonal prism at the bottom are about 150 and 200 nm, respectively.

To investigate how the third component affects the dielectric properties of composites, various contents of R-ZnO powders were mixed with BT + PVDF (f_{BT} = 0.30) to form R-ZnO/(BT + PVDF) composites by a hot-press procedures. The SEM image of composite in Figure 1 shows good dispersion of BT and R-ZnO nanostructures in the polymer. The inorganic interface between R-ZnO and BT

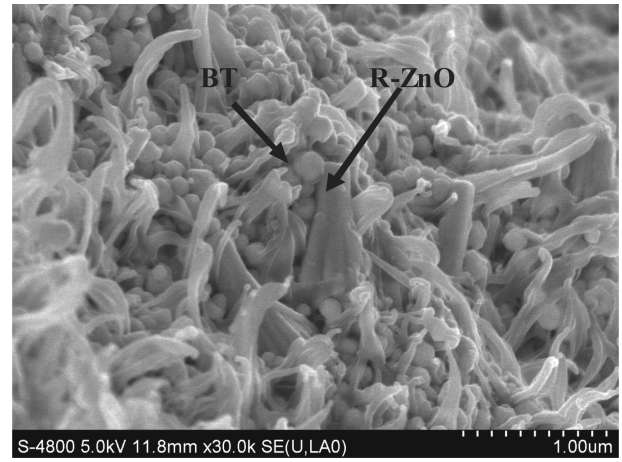

FIGURE 1. SEM micrographs of fractured surface of the R-ZnO/(BT + PVDF) composite with the R-ZnO content of 0.1705.

is also present, which may enhance the dielectric constant. The R-ZnO is basically kept in radial shape in the composites.

Compared with BT + PVDF composite, surprising dielectric properties are observed for R-ZnO/(BT + PVDF) composites because of the special nanostructure of R-ZnO. The dielectric constant of the BT + PVDF composite is improved obviously (shown in Figure 2a), and a low percolation threshold is observed for R-ZnO/(BT + PVDF) composites. The addition of R-ZnO can greatly improve the dielectric constant of BT + PVDF (25, 1×10^2 Hz) composites. This implies that the incorporation of ZnO nanowires clusters into BT + PVDF is very effective to increase its dielectric constant. The dielectric constant of R-ZnO/(BT + PVDF) composite increases nonlinearly with the increasing volume ratio; when the volume ratio is 0.17, the dielectric constant reaches its maximum of 175. The dielectric constant of composites decreases with increasing frequency from 1×10^2 Hz to 1 MHz, and it can still remain above 30 even at a high frequency as 1 MHz.

Additionally, the dielectric constant of the composite with R-ZnO is always larger than that of BT + PVDF composite. The variation of dielectric constant with the concentration of R-ZnO can be divided into three stages. Initially, the dielectric constant rises gradually with the increasing R-ZnO contents in the composites, because of the formation of new microcapacitance structures at low content of R-ZnO. Subsequently, the percolation threshold is visible, at a critical volume concentration $f_{R\text{-}ZnO}$ = 0.17, where the dielectric constant abruptly increases. At this stage, the conduction behavior of the composites is also controlled by the concentration of the conducting R-ZnO phase. Finally, the dielectric constant decreases because of a significant conductive network formation. The conductive network makes the composite become the conducting material and this leads to a high leakage current in the composite, so the dielectric constant decreases. The dielectric constant of R-ZnO/(BT + PVDF) composite increases nonlinearly with the increasing volume ratio, and when the volume ratio is 0.17, the dielectric constant reaches its maximum.

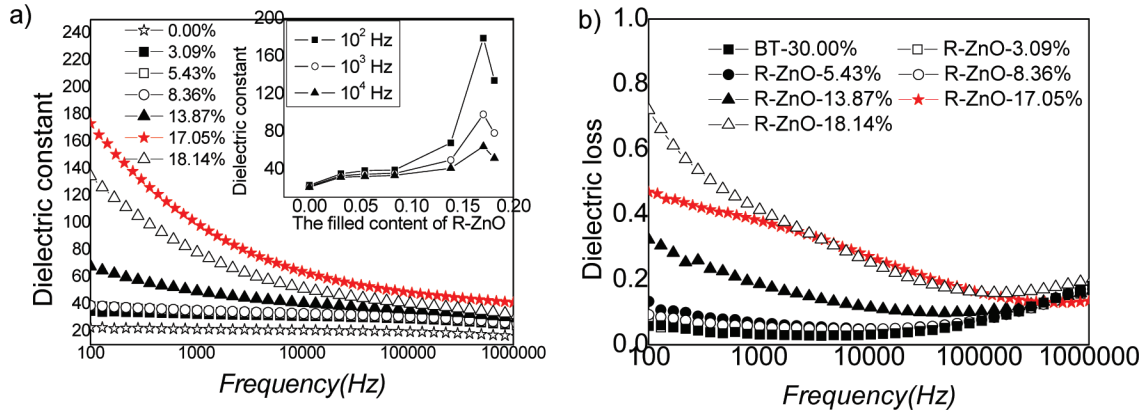

FIGURE 2. Dielectric constant and dielectric loss vs different frequencies for the R-ZnO/(BT + PVDF) composites with various R-ZnO volume ratios at room temperature: (a) Dielectric constant; inset is the change in dielectric constant with the filled content of R-ZnO at 1×10^2 Hz, 1×10^3 Hz, 1×10^4 Hz. (b) Dielectric loss.

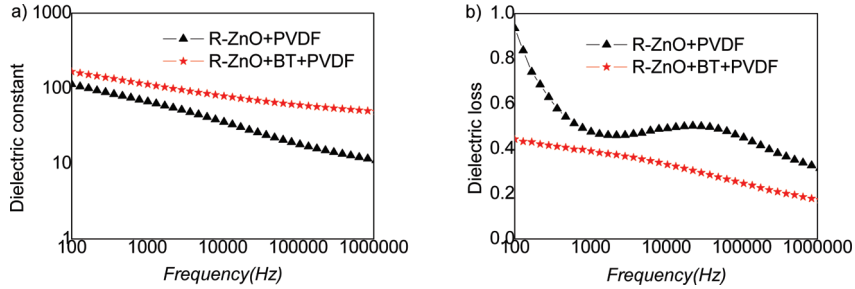

FIGURE 3. Comparison of (a) dielectric constant and (b) dielectric loss of R-ZnO/PVDF and R-ZnO/(BT + PVDF) composites in the neighbor of percolation threshold.

The variation in the dielectric loss vs frequencies for R-ZnO/(BT + PVDF) composites with various R-ZnO volume ratios is shown in Figure 2b. It is worth noting that the dielectric loss of the percolation R-ZnO/(BT + PVDF) composite at room temperature is as high as 0.4 in the frequency range of 1×10^2 to 1×10^3Hz, but at higher frequencies, the dielectric loss of the percolation composite decreases to lower than 0.2. Though the dielectric loss increases with further increasing frequency, it is still in an acceptable range in applications. Compared with the two-phase-percolative R-ZnO/PVDF composite at the percolation threshold (17), the dielectric constant of R-ZnO/ (BT + PVDF) composite is higher at all measured frequency (especially at high frequency), and less dependent on the frequency (shown in Figure 3a). And moreover, the dielectric loss is lower than that of R-ZnO/PVDF at all measured frequency (shown in Figure 3b). The increased dielectric constant and decreased dielectric loss of the three-phase-percolative composite implies that it is effective to increase the dielectric properties of the two-phase-percolative composites in the present composite system. The dielectric constant of R-ZnO/(BT + PVDF) composite at the frequency 1×10^4 Hz is almost two times higher than that of the BT + PVDF composite reported (7, 8), but the dielectric loss of R-ZnO/(BT + PVDF) composite is also higher than that of the BT + PVDF composite. Usually, the introduction of inorganic fillers to a polymer-matrix enhances the dielectric loss values of the composites, as there is an enhancement in the sources of charge carriers in the system induced by the electrically conductive R-ZnO (17).

The enhancement in the dielectric constant can be explained according to the percolation theory (18−20)

$$\varepsilon = \varepsilon_0 \left| \frac{f_c - f_{\text{R-ZnO}}}{f_c} \right|^{-q} \qquad (1)$$

Where ε_0 is the dielectric constant of the thermoplastic-ceramic matrix (BT+PVDF), $f_{\text{R-ZnO}}$ is the volume ratio of the R-ZnO, f_c is the percolation threshold, and q is a critical exponent of about 1. The experimental values of the dielectric constant are in good agreement with eq 1, with $f_c \approx 0.1723$ and $q \approx 0.9993$, but it is much higher than that of R-ZnO/PVDF composites ($f_c = 0.0661$). For the three-phase polymer-based materials, the percolation value is higher than that of the two-phase, which was also reported by Dang (21, 22). In the three-phase-percolative composites, the R-ZnO with the large aspect ratio and upright shape is the conducting filler. In the present system, we take into consideration some other reasons, like the snapped radial structure, which may be the main reason for the increased percolation threshold. Concretely, it can be concluded as follows (23, 24)

$$f_c = 1 - \exp[-B_c V / \langle V_{ex} \rangle] \qquad (2)$$

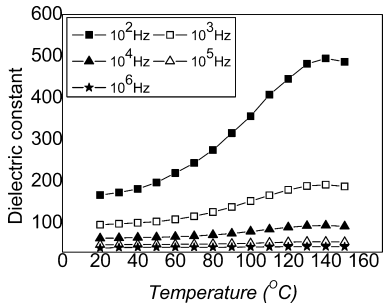

FIGURE 4. Temperature dependence of dielectric constant of the percolation R-ZnO/(BT + PVDF) composite and PVDF at different frequencies.

Where $-B_cV/\langle V_{ex}\rangle$ is the density number of the radial structure, V is the volume of the radial structure, $\langle V_{ex}\rangle$ is the exclude volume (volume of the overlapped radial structure), and B_c is the coefficient corresponding to the radial structure. For the radial structure composed of nanorods, the volume of the structure is expressed as (25−27)

$$V = \pi r^2 l \text{ and } V_{ex} = \pi l^2 r$$
$$f_c \approx B_c r/l \quad (3)$$

Where r is the diameter of the nanorod, l is the length of the nanorod. When the radial nanostructure overlapped, l would decrease. Seen from eq 3, f_c would increase with decreasing l, which confirms that the overlapped radial structure is critical for the increase of f_c.

Temperature dependence of the dielectric constant for the three-phase-percolative composite with $f_{R\text{-}ZnO} = 0.17$ is shown in Figure 4. The composite exhibits a good thermal stability at the frequency above 1×10^4 Hz. At low frequency, the molecules have enough time to be polarized, whereas at high frequency, the polarization of molecules does not have enough time to catch up with the change of applied electrical field, and thus the composite shows weak dependence of dielectric constant on temperature. Particularly, at 1×10^2 Hz, the dielectric constant increases from 180 to 500 when the temperature changes from 20 to 140 °C, and then decreases to 490. The temperature-dependent dielectric behavior of the composite can be explained as follows: With the increase in temperature, the composite becomes flexible and the movement of molecules is easier. However, the dielectric constant began to drop at above 140 °C. The PVDF melting process starts at 130 °C, after which the composite becomes flowing and the movement of molecules is greatly enhanced. The percolation in the composite then disappears at temperatures above 140 °C, with the percolation path being destroyed because of a large thermal expansion.

4. CONCLUSIONS

In summary, a three-phase-percolative R-ZnO/(BT + PVDF) composite has been prepared using a simple blending and hot-molding technique. Comparing with the R-ZnO/PVDF composites, the dielectric behavior is improved in three-phase-percolative composites. The increased percolation threshold has been explained in detail. High dielectric constant, reduced dielectric loss, and good thermal stability make the three-phase-percolative composites particularly attractive for practical applications.

Acknowledgment. The work was supported by the National Science Foundation for Postdoctoral Scientists.

REFERENCES AND NOTES

(1) Lu, J. X.; Wong, C. P. *IEEE Trans. Dielectr. Electr. Insul.* **2008**, *15*, 1322.
(2) Chan, H. L. W.; Cheung, M. C.; Choy, C. L. *Ferroelectrics* **1999**, *224*, 113.
(3) Gregorio, R.; Cestari, M.; Bernardino, F. E. *J. Mater. Sci.* **1996**, *31*, 2925.
(4) Rao, Y.; Ogitani, S.; Kohl, P.; Wong, C. P. *J. Appl. Polym. Sci.* **2002**, *83*, 1084.
(5) Dang, Z. M.; Lin, Y. H.; Nan, C. W. *Adv. Mater.* **2003**, *15*, 1625.
(6) Cho, S. D.; Lee, J. Y.; Hyun, J. G.; Paik, K. W. *Mater. Sci. Eng., B* **2004**, *110*, 233.
(7) Kułek, J.; Szafraniak, I.; Hilczer, B.; Połomska, M. *J. Non-Cryst. Solids* **2007**, *353*, 4448.
(8) Kobayashi, Y.; Tanase, T.; Tabata, T.; Miwa, T.; Konno, M. *J. Eur. Ceram. Soc.* **2008**, *28*, 117.
(9) Wang, L.; Dang, Z. M. *Appl. Phys. Lett.* **2005**, *87*, 042903.
(10) Dang, Z. M.; Wang, L.; Yin, Y.; Zhang, Q.; Lei, Q. Q. *Adv. Mater.* **2007**, *19*, 852.
(11) Qi, L.; Lee, B. I.; Chen, S.; Samuels, W. D.; Exarhos, G. J. *Adv. Mater.* **2005**, *17*, 1777.
(12) Lu, J.; Moon, K. S.; Xu, J.; Wong, C. P. *J. Mater. Chem.* **2006**, *16*, 1543.
(13) Xu, J. X.; Wong, C. P. *Appl. Phys. Lett.* **2005**, *87*, 082907.
(14) Dang, Z. M.; Shen, Y.; Nan, C. W. *Appl. Phys. Lett.* **2002**, *81*, 4814.
(15) Choi, H. W.; Heo, Y. W.; Lee, J. H.; Kim, J. J.; Lee, H. Y.; Park, E. T.; Chung, Y. K. *Appl. Phys. Lett.* **2006**, *89*, 132910.
(16) Xu, J. X.; Wong, C. P. *Proceedings of the 54th IEEE Electronic Components and Technology Conference*; IEEE: Piscataway, NJ, 2004; pp 536−541.
(17) Wang, G. S.; Deng, Y.; Xiang, Y.; Guo, L. *Adv. Funct. Mater.* **2008**, *18*, 2584.
(18) Nuzhnyy, D.; Petzelt, J.; Rychetsky, I.; Buscaglia, V.; Buscaglia, M. T.; Nanni, P. *J. Phys. D: Appl. Phys.* **2009**, *42*, 155408.
(19) Tagantsev, A. K.; Sherman, V. O.; Astafiev, K. F.; Venkatesh, J.; Setter, N. *J. Electroceram.* **2003**, *11*, 5.
(20) Nan, C. W. *Prog. Mater. Sci.* **1993**, *37*, 1.
(21) Dang, Z. M.; Wu, J. P.; Xu, H. P.; Yao, S. H.; Jiang, M. J. *Appl. Phys. Lett.* **2007**, *91*, 072912.
(22) Dang, Z.-M.; Fan, L.-Z.; Shen, Y.; Nan, C.-W. *Chem. Phys. Lett.* **2003**, *369*, 95.
(23) Balberg, I. *Phys. Rev. B* **1985**, *31*, 4053.
(24) Bug, A. L. R.; Safran, S. A.; Webman, I. D. *Phys. Rev. Lett.* **1985**, *55*, 1896.
(25) Pike, G. E.; Seager, C. H. *Phys. Rev. B* **1974**, *10*, 1421.
(26) Balberg, I.; Binenbaum, N.; Wagner, N. *Phys. Rev. Lett.* **1984**, *52*, 1465.
(27) Munson-McGee, S. H. *Phys. Rev. B* **1991**, *43*, 3331.

AM100296U